IEEE CSC & ESAS SUPERCONDUCTIVITY NEWS FORUM (global edition), February 2019.
Invited poster presentation 4LPo1H-02 given at ASC 2018, October 28-November 5, 2018, Seattle (USA).

Dynamic Breakdown Characteristics of Pancake Coil Model for Resistive Superconducting Fault Current Limiters

N. Hayakawa, *Member, IEEE,* M. Mimbu, H. Kojima, *Member, IEEE,* S. Isojima, and M. Kuwata

***Abstract*— Toward the reliable and rational insulation design of resistive superconducting fault current limiters (RSFCL), we have been investigating not only the intrinsic breakdown (BD) characteristics of liquid nitrogen (LN_2) without bubbles but also the dynamic BD characteristics of LN_2 under the transient bubble disturbance at the quench of RSFCL coils. We have so far used a fundamental model such as sphere-plane electrode system with quasi-uniform electric field. However, when RSFCL will be introduced in a future electric power network, a stack of pancake coils with non-uniform electric field will be adopted for the practical development of RSFCL. In this paper, we designed and fabricated a pancake coil model for RSFCL, and investigated the intrinsic and dynamic BD characteristics of the pancake coil models in LN_2. Experimental results are discussed in terms of the volume effect of intrinsic and dynamic BD strength under non-uniform electric field.**

***Index Terms*— bubble, electrical insulation, pancake coil, quench, superconducting fault current limiter**

I. Introduction

RESISTIVE superconducting fault current limiters (RSFCL) have been investigated and developed as one of the promising power apparatus for the protection of future electric power system in high density demand area [1]–[4]. By introducing RSFCL into the power system, it is possible to rapidly and effectively limit the fault current and enhance the transient stability of the power system [5]. When RSFCL operates, a quench of high-temperature superconducting (HTS) tapes will occur and generate bubbles transiently in LN_2. As the result, breakdown (BD) can be induced in LN_2 with the bubble disturbance under the operating voltage of RSFCL. We call such BD "dynamic BD", which is crucial together with the "intrinsic BD" without bubbles.

Since the bubble disturbance in operating RSFCL is transient during the quench and fault current limitation, the dynamic BD characteristics of LN_2 are essential for the rational insulation design of RSFCL. However, most of researches have investigated the BD characteristics of LN_2 with continuously generated bubbles [6]–[8]. We have suggested a flowchart of insulation design of RSFCL based on the intrinsic and dynamic BD characteristics, as shown in Fig. 1 [9]. Researches on dynamic BD have been carried out using a fundamental model such as sphere-plane electrode system with quasi-uniform electric field [9]–[12]. However, the practical RSFCL will have a structure with a stack of pancake coils, where a non-uniform electric field will be critical at the edges of HTS tapes and coils. Therefore, it is necessary to investigate the dynamic BD characteristics of LN_2 using a pancake coil model with non-uniform electric field for the reliable and rational insulation design of RSFCL.

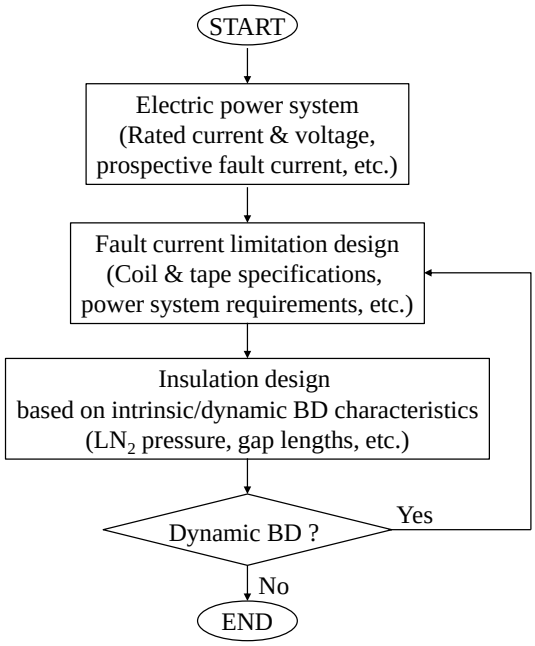

Fig. 1. Flowchart of insulation design for RSFCL [9].

In this paper, we designed and fabricated a pancake coil model for RSFCL using the bifilar nichrome tapes instead of HTS tapes, and investigated the intrinsic and dynamic BD characteristics of the pancake coil models in LN_2 for different gap length and vertical or horizontal arrangement of stack. Moreover, we systematized the experimental results in terms of the volume effect of intrinsic and dynamic BD strength under non-uniform electric field.

This work was supported in part by JSPS KAKENHI Grant Number JP17H03215.

N.Hayakawa, M.Mimbu, H.Kojima are with the Department of Electrical Engineering, Nagoya University, Nagoya 464-8603, Japan (e-mail: nhayakaw@nuee.nagoya-u.ac.jp, kojima@nuee.nagoya-u.ac.jp).

S.Isojima is with Sumitomo Electric Industries, Ltd., Osaka 554- 0024, Japan (e-mail: isojima-shigeki@sei.co.jp).

M.Kuwata is with Nissin Electric Co., Ltd., Kyoto 615-8686, Japan (e-mail: Kuwata_Minoru@nissin.co.jp).

II. Experimental Setup and Methods

The experimental setup is shown in Fig. 2. The cryostat has a FRP capacitor bushing, which is partial discharge (PD) free at 150 kV_{rms} in LN_2. Fig. 3(a) shows the pancake coil model as the first and main sample in this paper. The coil is bifilarly wound by two nichrome tapes with 4 mm width × 0.3 mm thickness instead of HTS tapes, and connected to the high voltage and grounded electrodes, respectively, with 3 turns and the gap length g of 2 mm or 6 mm between the adjacent tapes. The tapes are supported by FRP spacers with 25 mm height × 10 mm width × 2 or 6 mm thickness. The tape of grounded side also acts as a heater to generate bubbles transiently by the thyristor-controlled switch. The coil is sandwiched between FRP plate and PET plate to observe the bubble behavior, and arranged vertically or horizontally, as shown in Fig. 3(b). Fig. 4 shows the Turn-Turn model as the second sample simplifying the pancake model with g = 2 mm and 3–5 spacers.

In the above electrode systems, we carried out the following two kinds of BD tests for different gap length and vertical or horizontal arrangement of stack in LN_2 at the temperature of 77 K and the pressure of 0.1 MPa.

1) *Intrinsic BD test without bubbles*

AC high voltage of 60 Hz was applied to the tape of high voltage side at the increasing rate of 1 kV_{rms}/s, until the BD occurs without bubbles. The BD voltage was measured 20 times repeatedly at the same condition. The intrinsic BD voltage $V_{intrinsic}$ with 50 % probability was calculated by the Weibull analysis, and converted to the intrinsic BD strength $E_{intrinsic}$ with 50 % probability at the tape edges.

2) *Dynamic BD test with transient bubble disturbance*

At the applied voltage V_a below $V_{intrinsic}$, the tape of grounded side was energized to generate bubbles with the heater power density of 5 W/cm^2. Bubbles were generated 20 times repeatedly at a fixed V_a, and the generation probability of dynamic BD was obtained. This operation was repeated for different V_a to get the dynamic BD probability at each V_a. The dynamic BD strength $E_{dynamic}$ with 50 % probability was calculated by the relationship between the BD probability and V_a.

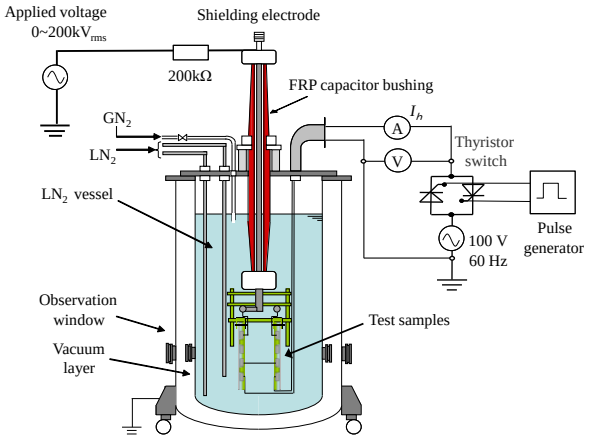

Fig. 2. Experimental setup.

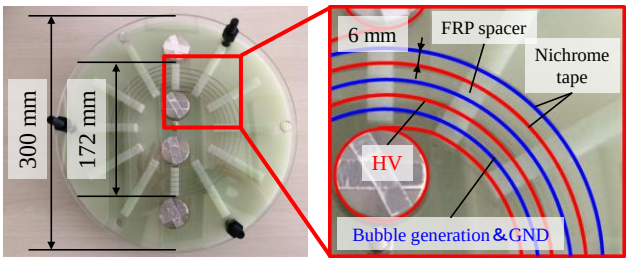

(a) Electrode configuration

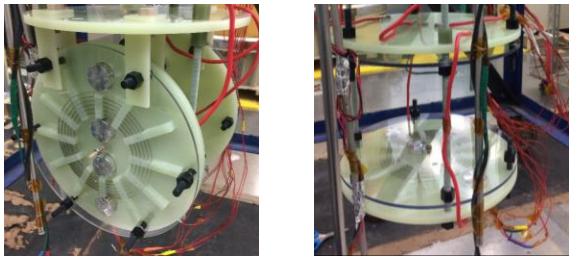

Vertical Horizontal

(b) Arrangement of pancake coil model

Fig. 3. Pancake coil model.

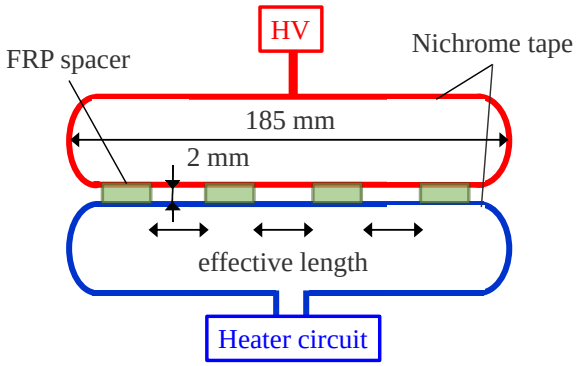

Fig. 4. Turn-Turn model. Number of spacer is 4.

Table I summarizes the test samples and test conditions, which includes our previous data under sphere-plane electrodes [11], [13], the other researchers' data [12], [14]. Fink at KIT investigated the intrinsic and dynamic BD for sphere-plane electrode, as shown in Fig. 5, under quasi-uniform and non-uniform electric fields [12]. Humpert at TH Köln investigated the intrinsic BD for tip-plane electrode, as shown in Fig. 6, under non-uniform electric field [14]. The field utilization factor ζ of the pancake coil model and the Turn-Turn model was calculated with the simplified 2-dimensional model with the tape edge radius of 0.01 mm and the minimum mesh size of 0.002 mm, without considering the spacer.

TABLE I
Test Samples for Various Researchers

Organization	Electrode configuration	Diameter ϕ [mm]	Gap length g [mm]	Field utilization factor ζ	Temperature T [K]	Pressure P [MPa]
Nagoya University	Sphere-plane [11][13]	6, 20, 50	0.5–8	0.396–0.986	65–77	0.1–0.3
	Turn-Turn	-	2	0.187	77	0.1
	Pancake coil	-	2–6	0.090–0.153	77	0.1
KIT [12]	Sphere-plane	50	2–90	0.251–0.949	77	0.1
TH Köln [14]	Tip-plane	1, 2, 4	10–50	0.006–0.233	77	0.1–0.3

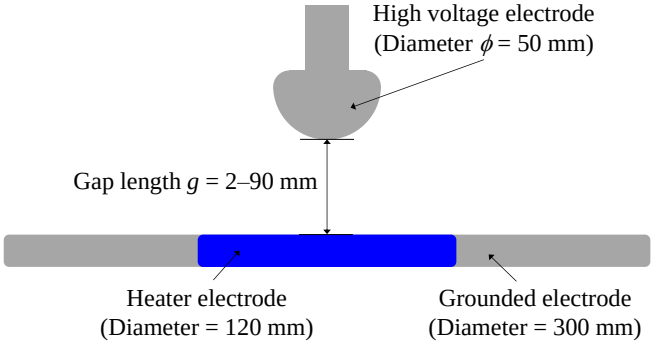

Fig. 5. Electrode configuration of KIT [12].

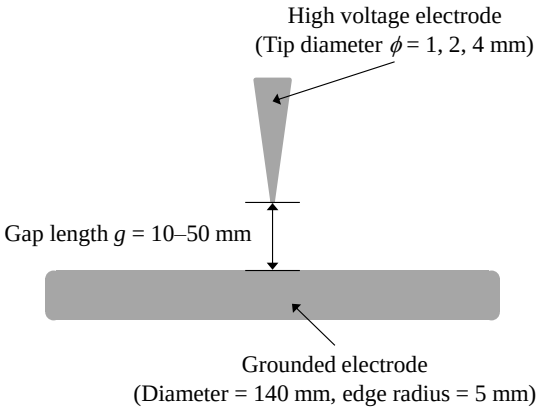

Fig. 6. Electrode configuration of TH Köln [14].

III. Experimental Results and Discussion

A. Spacer Number Dependence of Breakdown Strength in Turn-Turn Model

FRP spacer surfaces between adjacent tapes may become weak points on electrical insulation in LN_2. Fig. 7 shows the spacer number dependence of $E_{intrinsic}$ and $E_{dynamic}$ in the Turn - Turn model with g = 2 mm. The error bars represent the standard deviation. $E_{dynamic}$ was about 23 % lower than $E_{intrinsic}$. $E_{intrinsic}$ and $E_{dynamic}$ increased slightly with the increase in the spacer number or the decrease in the effective length with the sharp edges of tapes in LN_2. In addition, we confirmed that the discharge occurred not only on the spacer surface but also at the gap between the tapes in LN_2. These results suggest that FRP spacer surfaces may not be major weak points on the electrical insulation of Turn-Turn model at g = 2 mm.

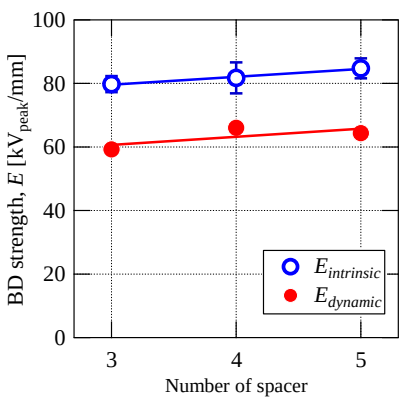

Fig. 7. Intrinsic BD strength $E_{intrinsic}$ and dynamic BD strength $E_{dynamic}$ in Turn-Turn model as a function of the number of spacer. g = 2 mm.

B. Gap Length Dependence of Breakdown Strength in Pancake Coil Model

Fig. 8 shows the gap length dependence of $E_{intrinsic}$ and $E_{dynamic}$ in the pancake coil model arranged vertically. $E_{intrinsic}$ decreased with the increase in the gap length, which can be attributed to the volume effect of BD strength in LN_2 [13] in the pancake coil model. On the other hand, $E_{dynamic}$ was lower than $E_{intrinsic}$, but increased with the increase in the gap length. $E_{dynamic}$ / $E_{intrinsic}$ increased from 0.86 at g = 2 mm to 0.96 at g = 6 mm, which suggests that the longer gap length contributes to the improvement of the dynamic BD characteristics [11] even under non-uniform electric field such as the pancake coil model.

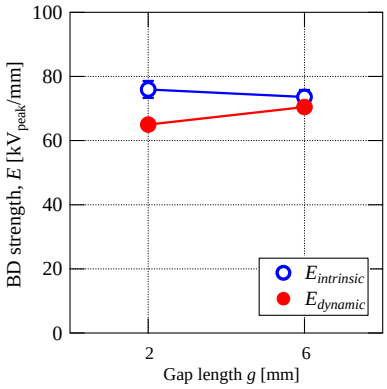

Fig. 8. Gap length dependence of intrinsic BD strength $E_{intrinsic}$ and dynamic BD strength $E_{dynamic}$ in pancake coil model of vertical arrangement.

C. Breakdown Strength of Pancake Coil Model for Vertical or Horizontal Arrangement

Fig. 9 shows $E_{intrinsic}$ and $E_{dynamic}$ in the pancake coil model with g = 6 mm for different coil arrangement. Both $E_{intrinsic}$ and $E_{dynamic}$ of horizontal arrangement are lower than those of vertical arrangement. The decrease of $E_{dynamic}$ is remarkable than that of $E_{intrinsic}$. In the vertical arrangement, the generated bubbles can escape from the high field area due to the buoyancy. On the other hand, in the horizontal arrangement, the generated bubbles are difficult to escape due to the upper PET plate, and remain in the high field area. This means that the vertical arrangement will be better for RSFCL in consideration of the dynamic BD characteristics.

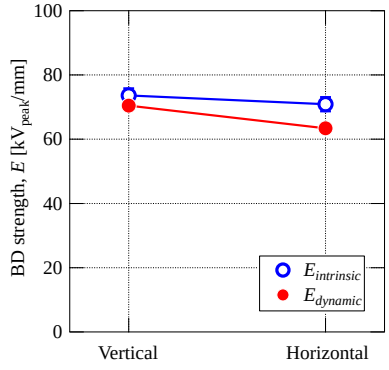

Fig. 9. Intrinsic BD strength $E_{intrinsic}$ and dynamic BD strength $E_{dynamic}$ in pancake coil model for different arrangement directions. g = 6 mm.

D. Volume Effect of Breakdown Strength under Non-Uniform Electric Field

We have revealed that $E_{intrinsic}$ and $E_{dynamic}$ of LN_2 can be systematized in terms of the volume effect under quasi-uniform electric field of $\zeta > 0.6$ with sphere-plane electrode, as shown in Fig. 10 [11], [13]. α%SLV on the horizontal axis means the stressed liquid volume (SLV) with the BD strength higher than α (%) of the maximum strength E_{max}. The value of α depends on the temperature and pressure of LN_2, e.g. α = 81 % at 77 K, 0.1 MPa, and α = 93 % at 65 K, 0.3 MPa [13]. α%SLV can be calculated by electric field analysis using COMSOL Multiphysics with the following process:

1) Calculate E_{max} by electric field analysis.
2) Pick up the meshes with the electric field strength E_a at each mesh greater than α × E_{max}.
3) Integrate the volume or area of the meshes picked up at 2) as α%SLV.

Fig. 11 shows the examples to calculate α%SLV for sphere-plane electrode and pancake coil model. In Fig. 10, $E_{intrinsic}$ decreases within the prediction interval of 95 % with the increase in α%SLV. $E_{dynamic}$ are lower than the bottom line of the prediction interval of $E_{intrinsic}$ and decreased with the increase in α%SLV.

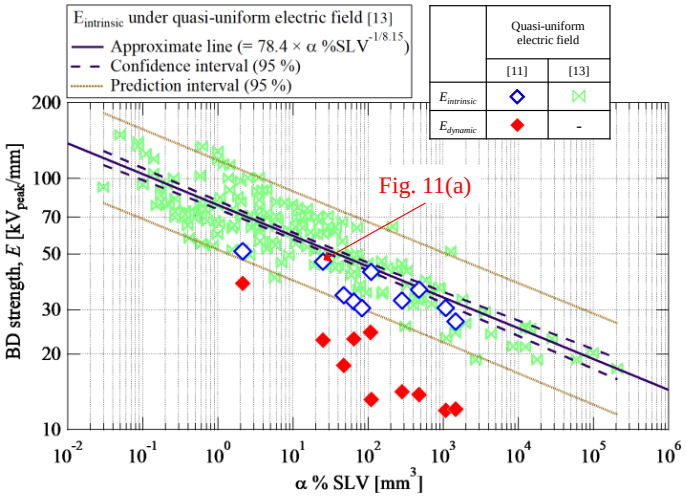

Fig. 10. Volume effect of intrinsic BD strength $E_{intrinsic}$ and dynamic BD strength $E_{dynamic}$ in LN_2 under quasi-uniform electric field of $\zeta > 0.6$ [11].

In this section, we introduce $E_{intrinsic}$ and $E_{dynamic}$ of LN_2 under non-uniform electric field of $\zeta < 0.6$ in the previous sections and the other researchers' data into Fig. 10, in order to systematize the volume effect of $E_{intrinsic}$ and $E_{dynamic}$ of LN_2 under both quasi-uniform and non-uniform electric field.

1. Intrinsic breakdown strength $E_{intrinsic}$

Fig. 12 shows the gap length dependence of $E_{intrinsic}$ and $E_{dynamic}$ in LN_2 with sphere-plane electrode based on the data by KIT [12]. In addition, Fig. 13 shows the gap length dependence of $E_{intrinsic}$ in LN_2 with tip-plane electrode based on the data by TH Köln [14]. Fig. 14 summarizes $E_{intrinsic}$ not only in Figs. 7–9 and [11] but also in Fig. 12 and Fig. 13. α%SLV under non-uniform electric field are smaller than those under quasi-uniform electric field, since

Test sample	Sphere-plane
T [K]	77
P [MPa]	0.1
α [%]	81
ϕ [mm]	20
g [mm]	2
V_a [kV_{peak}]	82.1
ζ	0.877

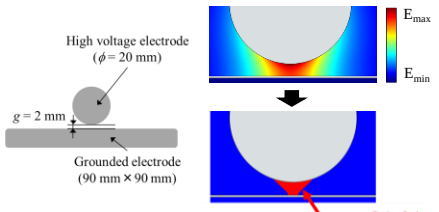

1) Calculate E_{max} by electric field analysis with minimum mesh size of 0.1 mm (2D axis object). ➡ E_{max} = 46.6 kV_{peak}/mm
2) Pick up the meshes with the electric field strength E_a at each mesh greater than 0.81 × 46.6 = 37.7 kV_{peak}/mm.
3) Integrate the volume of the meshes picked up at 2) in axisymmetric system. ➡ α%SLV = 25.7 mm^3

(a) Sphere-plane model (ϕ = 20 mm, g = 2 mm, Fig. 10)

Test sample	Pancake coil
T [K]	77
P [MPa]	0.1
α [%]	81
g [mm]	2
V_a [kV_{peak}]	23.2
ζ	0.187

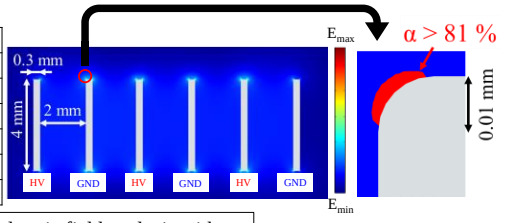

1) Calculate E_{max} by electric field analysis with minimum mesh size of 0.002 mm (2D object). ➡ E_{max} = 76.0 kV_{peak}/mm
2) Pick up the meshes with the electric field strength E_a at each mesh greater than 0.81 × 76.0 = 61.6 kV_{peak}/mm.
3) Integrate the area (1.5E-4 mm^2) of the meshes picked up at 2) and multiply the coil length (1808 mm, measured). ➡ α%SLV = 0.27 mm^3

(b) Pancake coil model (g = 2 mm, Fig. 14)

Fig. 11. Calculation process of α%SLV.

the highly stressed region is limited around the tape edges or the tips. $E_{intrinsic}$ under non-uniform electric field decreased with the increase in α%SLV within the prediction interval of 95 % obtained under quasi-uniform electric field. This result means that $E_{intrinsic}$ without bubbles can be systematized in terms of the volume effect of BD strength in LN_2 under both quasi-uniform and non-uniform electric field.

2. Dynamic breakdown strength $E_{dynamic}$

Fig. 15 summarizes $E_{dynamic}$ not only in Figs. 7–9 and [11] but also in Fig. 12. $E_{dynamic}$ were near or lower than the bottom line of the prediction interval of $E_{intrinsic}$ and decreased with the increase in α%SLV even under non-uniform electric field as well as under quasi-uniform electric field. Therefore, the volume effect can also be confirmed in $E_{dynamic}$ with transient bubbles under both quasi-uniform and non-uniform electric field.

From the above, we suggest that $E_{dynamic}$ is lower than $E_{intrinsic}$ and the volume effect of $E_{intrinsic}$ and $E_{dynamic}$ can be applied, regardless of the quasi-uniform/non-uniform electric field and with/without transient bubbles. The reliable and rational insulation design of RSFCL based on $E_{intrinsic}$ and $E_{dynamic}$ can be expected in consideration of their volume effect.

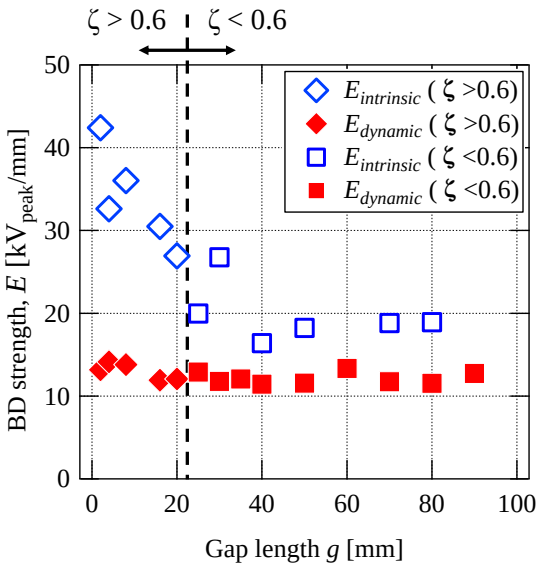

Fig. 12. Gap length dependence of intrinsic BD strength $E_{intrinsic}$ and dynamic BD strength $E_{dynamic}$ at sphere-plane electrode by KIT. Sphere diameter ϕ = 50 mm [12].

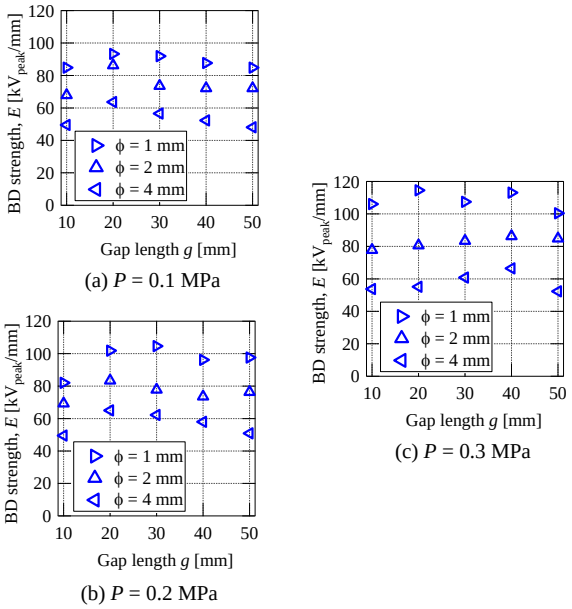

Fig. 13. Gap length dependence of intrinsic BD strength $E_{intrinsic}$ for different tip diameter and LN_2 pressure at tip-plane electrode by TH Köln [14].

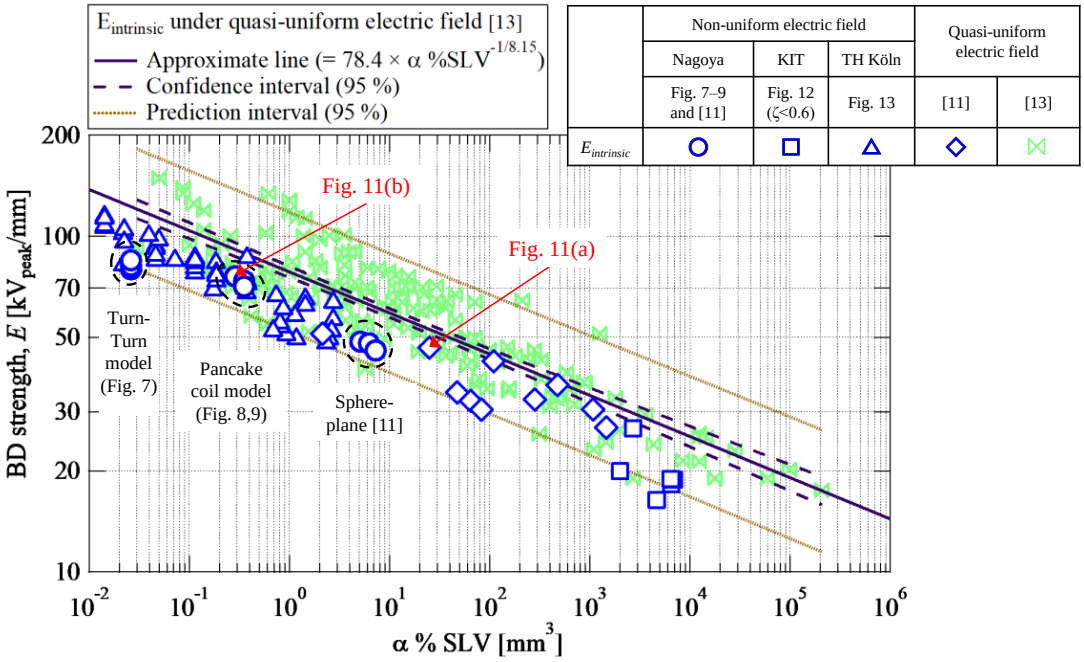

Fig. 14. Volume effect of intrinsic BD strength $E_{intrinsic}$ in LN_2 under quasi-uniform and non-uniform electric field.

IV. Conclusion

In this paper, we designed and fabricated a Turn-Turn model and a pancake coil model for the practical RSFCL and investigated the intrinsic and dynamic BD characteristics ($E_{intrinsic}$, $E_{dynamic}$) under non-uniform electric field in LN_2. Experimental results revealed the followings:

1) $E_{dynamic}$ with transient bubbles in LN_2 is lower than $E_{intrinsic}$ without bubbles.
2) $E_{intrinsic}$ and $E_{dynamic}$ can be estimated by the calculation of α%SLV in terms of the volume effect, regardless of the quasi-uniform/non-uniform electric field.
3) Based on $E_{intrinsic}$ and $E_{dynamic}$, the reliable and rational insulation design of RSFCL can be expected.

Acknowledgment

The authors would like to thank Mr. S. Fink at Karlsruhe Institute of Technology (KIT), Germany, and Prof. C. Humpert at Technische Hochschule (TH) Köln, Germany, for their valuable data and discussion.

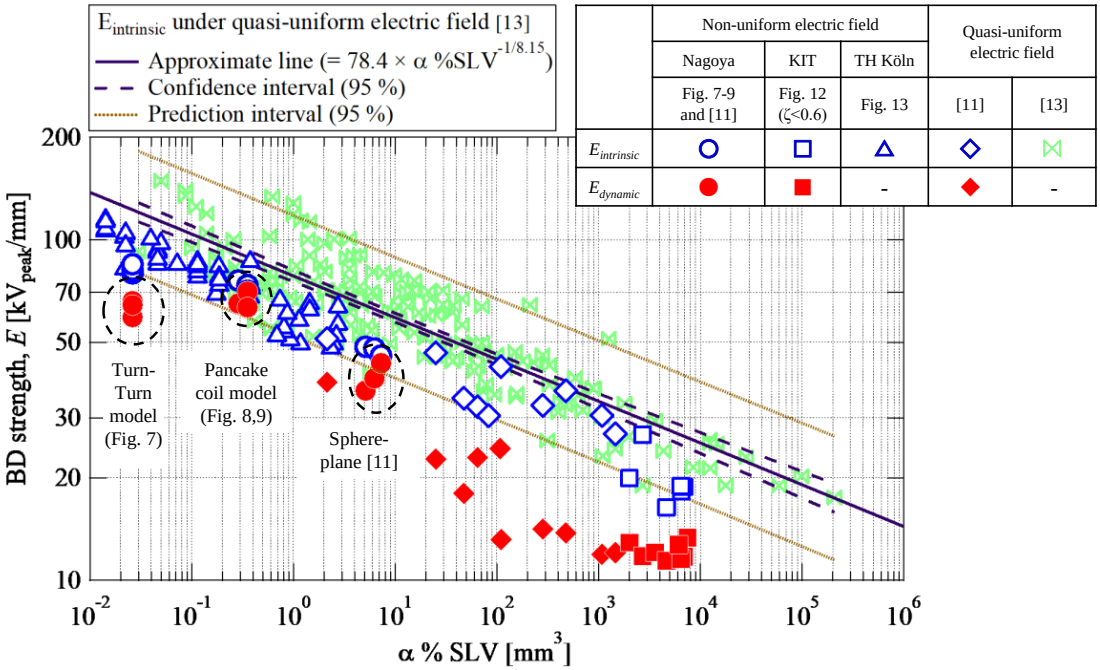

Fig. 15. Volume effect of intrinsic BD strength $E_{intrinsic}$ and dynamic BD strength $E_{dynamic}$ in LN_2 under quasi-uniform and non-uniform electric field.

REFERENCES

[1] A. Morandi, "Fault current limiter: an enabler for increasing safety and power quality of distribution networks," *IEEE Trans. Appl. Supercond.*, vol.23, no.6, 5604608, 2013.

[2] J. Bock, A. Hobl, J. Schramm, S. Krämer, and C. Jänke, "Resistive superconducting fault current limiters are becoming a mature technology," *IEEE Trans. Appl. Supercond.*, vol. 25, no. 3, 5600604, 2015.

[3] G. Angeli, M. Bocchi, M. Ascade, V. Rossi, A. Valzasina, and L. Martini, "Development of superconducting devices for power grids in Italy: update about the SFCL project and launching of the research activity on HTS cables", *IEEE Trans. Appl. Supercond.*, vol. 27, no. 4, 5600406, 2017.

[4] M. Moyzykh, D. Sotnikov, D. Gorbunova, and S. Samoilenkov, "Superconducting fault current limiter for Moscow 220 kV city grid," *European Conference on Applied Superconductivity 2017*, 1LO1-02, 2017

[5] N. Hayakawa, Y. Maeno, and H. Kojima, "Fault current limitation coordination in electric power grid with superconducting fault current limiters," *IEEE Trans. Appl. Supercond.*, vol. 28, No.4, 5602304, 2018.

[6] M. Hara, D. J. Kwak, and M. Kubuki, "Thermal bubble breakdown characteristics of LN_2 at 0.1 MPa under a.c. and impulse electric fields," *Cryogenics*, vol.29, pp.895–903, 1989.

[7] I. Sauers, R. James, A. Ellis, E. Tuncer, G. Polizos, and M. Pace, "Effect of bubbles on liquid nitrogen breakdown in plane-plane electrode geometry from 100-250 kPa," *IEEE Trans. Appl. Supercond.*, vol.21, no.3, pp.1892–1895, 2011.

[8] M. Blaz and M. Kurrat, "Influence of bubbles in pressurized liquid nitrogen on the discharge behavior in a homogeneous electric field," *IEEE Trans. Appl. Supercond.*, vol.23, 7700804, 2013.

[9] N. Hayakawa, T. Matsuoka, H. Kojima, S. Isojima, and M. Kuwata, "Breakdown characteristics and mechanisms of liquid nitrogen under transient thermal stress for superconducting fault current limiters," *IEEE Trans. Appl. Supercond.*, vol. 27, No.4, 7700305, 2017.

[10] N. Hayakawa, T. Matsuoka, K. Ishida, H. Kojima, S. Isojima, and M. Kuwata, "Pressure dependence and size effect of LN_2 breakdown characteristics under transient thermal stress," *IEEE Trans. Appl. Supercond.*, vol. 26, No.3, 7700604, 2016.

[11] N. Hayakawa, K. Ishida, M. Mimbu, H. Kojima, S. Isojima, and M. Kuwata, "Volume effect of dynamic breakdown strength in LN_2 for insulation design of resistive superconducting fault current limiters," *IEEE Trans. Appl. Supercond.*, vol. 28, No.4, 5600804, 2018.

[12] S. Fink, H.–R. Kim, R. Mueller, M. Noe, and V. Zwecker, "AC breakdown voltage of liquid nitrogen depending on gas bubbles and pressure," *Int. Conf. on High Voltage Engineering and Application*, 7035445, 2014.

[13] N. Hayakawa, S. Nishimachi, H. Kojima, and H.Okubo, "Size effect on breakdown strength in sub-cooled liquid nitrogen for superconducting power apparatus," *IEEE Trans. Dielectr. Electr. Insul.*, vol. 22, no. 5, pp. 2565–2571, 2015.

[14] C. Humpert, H. Seufert, R. Brustle, F. Kasten, G. Pfeiffer, and R. Schumacher, "Breakdown characteristics of liquid nitrogen in non-uniform electric fields," *Int. Conf. on Properties and Applications of Dielectric Materials*, No. 384, 2018